Optical Minimum-Shift Keying with Direct Detection (MSK/DD)

Michael Ohm and Joachim Speidel

Institute of Telecommunications, University of Stuttgart,
Pfaffenwaldring 47, 70569 Stuttgart, Germany

ABSTRACT

This paper presents a new optical Minimum-Shift Keying (MSK) modulation scheme with high spectral efficiency. The transmitter is realized in an Offset-Quaternary Phase-Shift Keying (QPSK) arrangement. The receiver uses a delay & add filter (DAF) and photodiodes for direct detection. An MSK precoder for the transmitter is derived.

Keywords: Optical communications, (continuous-)phase modulation, minimum-shift keying, direct detection

1. INTRODUCTION

Recently, several new modulation schemes for increasing spectral efficiency compared to intensity modulation (IM) or differential binary phase-shift keying (DBPSK) were proposed, e.g. differential quadrature phase-shift keying (DQPSK),[1] combined amplitude-/phase-shift keying (ASK-DPSK),[2] differential 8-level phase-shift keying (8-DPSK),[3] and optical QAM with orthogonal polarization (OQ^{2}AM).[4] They have a higher spectral efficiency because more than 1 bit/symbol as in IM or DBPSK is transmitted allowing for lower symbol rates. MSK belongs to the class of continuous-phase modulation (CPM) schemes and has an increased spectral efficiency compared to IM or DBPSK, although it is also a binary scheme. This is because the phase of the MSK signal is continuous over time and changes only along well-defined phase trajectories.[5] We present a transmitter for optical MSK based on two Mach-Zehnder modulators (MZM) similar to the transmitter for DQPSK.[1] The MSK receiver with one delay & add filter (DAF) and photodiodes for direct detection is similar to the DBPSK receiver.[6]

First, the basics of MSK are shortly reviewed in section 2. Then the MSK transmitter will be presented in section 3. After that, demodulation is analyzed and the proposed receiver will be shown in section 4. In section 5 an equivalent circuit for the MSK system will be given, which helps deriving the precoder function needed at the transmitter. Finally, features of optical MSK are investigated and compared to those of other optical modulation schemes in section 6.

2. MSK BASICS

The phase $\varphi(t)$ of a phase-shift keying (PSK) signal normaly exhibits discontinuities due to hard switching. This gives rise to a broad spectrum of PSK signals. In contrast, the phase of the MSK signal is a continuous time function.[5] The MSK signal is expressed in general as

$$e_{\mathrm{MSK}}(t) = A \cdot \sqrt{P} \cdot \exp\{\mathrm{j}[\omega_0 t + \varphi(t)]\}. \tag{1}$$

P is the constant power of the MSK signal and A is a constant factor. As can be seen from Fig. 1, $\varphi(t)$ is linear and the phase changes between consecutive sampling instants nT, $n \in \{0, \pm1, \pm2, \ldots\}$ are $\pm\pi/2$. A linear increase represents bit '1' and a linear decrease represents bit '0'. In Fig. 1. $\varphi(0) = 0$ is assumed.

Obviously, the time derivative of the continuous and piece wise linear phase $\varphi(t)$ is

Further author information: {ohm,speidel}@inue.uni-stuttgart.de; phone +49-711-685-8016; fax +49-711-685-7929

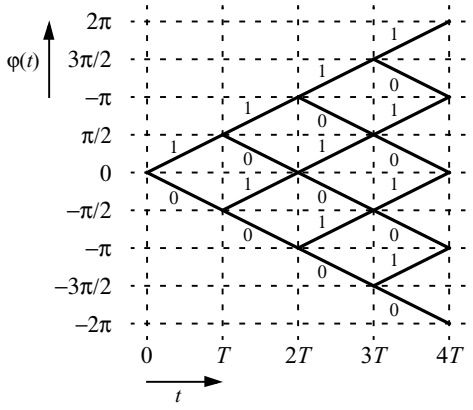

Figure 1. Phase trajectories of MSK

$$\frac{\partial \varphi}{\partial t} = \pm \frac{\pi}{2} \cdot \frac{1}{T}. \tag{2}$$

The instantaneous frequency of the MSK signal thus is

$$f_{m,0} = \frac{\omega_0}{2\pi} - \frac{1}{4T} \tag{3}$$

for bit '0' and

$$f_{m,1} = \frac{\omega_0}{2\pi} + \frac{1}{4T} \tag{4}$$

for bit '1'. The difference of the two instantaneous frequencies is

$$\Delta f_m = f_{m,1} - f_{m,0} = \frac{1}{2T}. \tag{5}$$

This is the minimum frequency separation of two signals in order to ensure their orthogonality over a symbol period T. Therefore the name of this modulation scheme is MSK.

3. OPTICAL MSK TRANSMITTER

3.1. Offset-QPSK

MSK can be implemented as offset-QPSK with cosine-impulse shaping.[5] The presented optical MSK modulator follows this idea. The baseband offset-QPSK signal is

$$s(t) = a(t) + \mathrm{j}b(t) = \sum_{n=-\infty}^{\infty} [q_{2n} \cdot g(t - 2nT) + \mathrm{j}q_{2n+1} \cdot g(t - 2nT - T)]. \tag{6}$$

q_k is the input symbol sequence to the modulator with $q_k = -1$ for bit '0' and $q_k = +1$ for bit '1'. The symbol sequence c_k shall be equivalent to q_k, such that $c_k = 1$ if $q_k = 1$ and $c_k = 0$ if $q_k = -1$ (thus $c_k \in \{0, 1\}$). It will be needed later. Symbols with even indices are transmitted via the in-phase component, the symbols with odd indices are transmitted via the quadrature component. The quadrature component is delayed ("offset") from the in-phase component by T. For MSK an impulse $g(t)$ is defined as

$$g(t) = w(t) \cdot \cos\left(\frac{\pi}{2} \cdot \frac{t}{T}\right) \tag{7}$$

with the window function

$$w(t) = \begin{cases} 1 & , \quad -T \leq t < T \\ 0 & , \quad \text{elsewhere} \end{cases} . \tag{8}$$

For the delayed impulse in the quadrature component follows

$$g(t-T) = w(t-T) \cdot \sin\left(\frac{\pi}{2} \cdot \frac{t}{T}\right). \tag{9}$$

$g(t)$ is shown in Fig. 2. Note, that its duration is twice the symbol duration. The MSK signal is now written as

$$\begin{aligned} e_{\text{MSK}}(t) &= A \cdot \sqrt{P} \cdot s(t) \cdot \exp(\text{j}\omega_0 t) \\ &= A \cdot \sqrt{P} \cdot |s(t)| \cdot \exp\{\text{j}[\omega_0 t + \varphi(t)]\}. \end{aligned} \tag{10}$$

It can be shown that $|s(t)| = 1$. The phase $\varphi(t)$ in (10) is

$$\varphi(t) = \arctan\left[\frac{b(t)}{a(t)}\right] = \arctan\left\{\frac{\sum_{n=-\infty}^{\infty} q_{2n+1} \cdot w(t-2nT-T) \cdot \sin\left[\frac{\pi}{2T}(t-2nT)\right]}{\sum_{n=-\infty}^{\infty} q_{2n} \cdot w(t-2nT) \cdot \cos\left[\frac{\pi}{2T}(t-2nT)\right]}\right\}. \tag{11}$$

As $q_k \in \{-1, 1\}$, the first part in the argument of the arctan-function determines the sign of the function, which can change only at the time instants mT, $m \in \{0, \pm 1, \pm 2, \ldots\}$, depending on the q_k. For evaluating (11) in time intervals of length T, the offset of in-phase and quadrature component has to be considered. The offset is illustrated in Fig. 3. For time intervals in which the index of q_k in the numerator is greater than the index of q_k in the denominator, the sign of the argument is q_k/q_{k-1}. For the time intervals in which the index of q_k in the numerator is smaller than the index of q_k in the denominator, the sign of the argument is $-q_k/q_{k+1}$. So the phase is

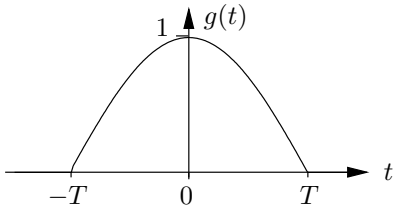

Figure 2. Cosine impulse $g(t)$ for MSK

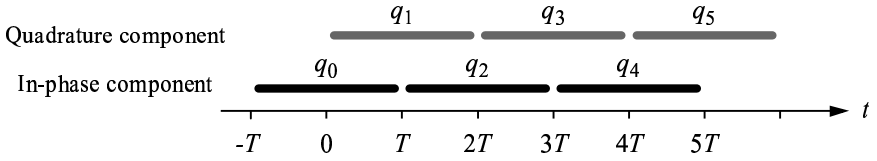

Figure 3. Offset of in-phase and quadrature components and relation between symbol sequence and time intervals

$$\varphi(t) = \pm \sum_{k=-\infty}^{\infty} w(2t - T/2 - kT) \cdot \frac{\pi}{2T} \cdot (t - kT) + \tilde{\varphi}(t). \tag{12}$$

In this representation $\tilde{\varphi}(t)$ ensures that $\varphi(t)$ is continuous. $\tilde{\varphi}(t)$ is constant over time intervals of length T. With $w(2t - T/2 - kT)$, pieces of length T are selected. Thus, MSK can be implemented as offset-QPSK.

3.2. Impulse shaping

As stated in section 3.1 cosine-impulse shaping is necessary for MSK modulation. This can be achieved with a MZM. The electrical field strength of the optical signal at the output of a MZM is[7]

$$e_{\text{out}} = e_{\text{in}} \cdot \cos\left(\pi \frac{v}{V_\pi}\right). \tag{13}$$

e_{in} is the field strength at the optical input of the MZM usually from a continuous-wave (CW) laser. v is the applied drive voltage, and V_π is the voltage that causes a phase shift of π in the arms of the modulator. The MZM transfer characteristic from 13 is plotted in Fig. 4. For a positive cosine envelope representing bit '1' the drive voltage has to rise linearly from $-V_\pi/2$ to $V_\pi/2$ or fall vice versa, and for a negative cosine envelope representing bit '0' the drive voltage has to go linearly from $V_\pi/2$ to $3V_\pi/2$ or vice versa. In order to get positive or negative cosine envelopes the drive voltage is composed of

$$v = v_1 + v_2. \tag{14}$$

$v_1(t)$ is a periodical triangular function independent of the data as illustrated in Fig. 5. Over a time span of $2T$ $v_1(t)$ it rises linearly from $-V_\pi/2$ to $V_\pi/2$ and falls to $-V_\pi/2$ during the next time span $2T$. $v_2(t)$ is the data signal. It is

$$v_{2,a}(t) = \sum_{n=-\infty}^{\infty} V_\pi \cdot \overline{c_{2n}} \cdot w(t - 2nT) \tag{15}$$

for the in-phase component and

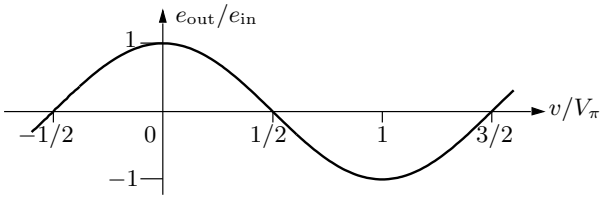

Figure 4. Transfer characteristic of Mach-Zehnder modulator

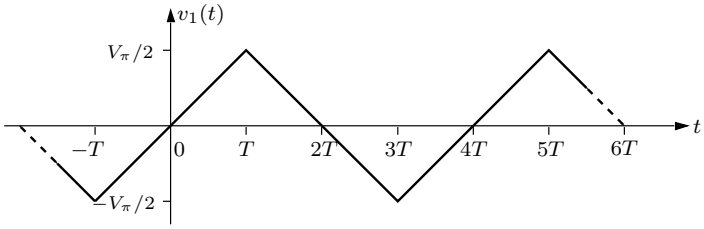

Figure 5. Periodic triangular drive voltage $v_1(t)$

$$v_{2,b}(t) = \sum_{n=-\infty}^{\infty} V_\pi \cdot \overline{c_{2n+1}} \cdot w(t - 2nT - T) \tag{16}$$

for the quadrature component. $\overline{c_k}$ is the inverted equivalent symbol sequence as described in section 3.1 with $c_k \in \{0, 1\}$. So $v_2(t)$ selects either the positive or the negative part of the MZM characteristic, while $v_1(t)$ is responsible for the cosine impulse shaping.

3.3. MSK transmitter

The MSK transmitter is shown in Fig. 6. Data symbols c_k with even indices are forwarded to the upper output (e), data symbols c_k with odd indices to the lower output (o) of the multiplexer. After inversion of the data symbols and rectangular (non-return to zero) impulse shaping we get the drive voltage $v_{2,a}(t)$ and with a delay element of delay T the drive voltage $v_{2,b}(t)$, respectively. The drive voltage $v_1(t)$ and its delay version $v_1(t - T)$ are generated separately. Light from a continuous-wave (CW) laser

$$e_{\mathrm{cw}}(t) = A \cdot \sqrt{P} \cdot \exp(\mathrm{j}\omega_0 t) \tag{17}$$

is split by a cross-coupler into two paths and then modulated by two MZM. ω_0 is the carrier angular frequency, P is the power of the CW laser and A a constant factor. At the output of the transmitter we have the desired MSK signal given in (10).

4. MSK RECEIVER

In this section an optical receiver for direct detection of the MSK signal according to (10) will be presented. We recall that the phase difference between two time instants mT and $(m+1)T$, $m \in \{0, \pm1, \pm2, \ldots\}$ is either $-\pi/2$ for bit '0' or $+\pi/2$ for bit '1' in the time span $mT \leq t < (m+1)T$. Thus, the MSK signal can be demodulated differentially with the receiver in Fig. 8. The MSK receiver consists of an optical DAF and an O/E converter with two photodiodes. With a phase shift $\psi = 3\pi/2$ in the lower branch and the delay $\tau = T$ in the upper branch of the DAF, the output current of the receiver becomes[3]

$$i_0(t) = K \cdot R \cdot P \cdot A^2 \cdot \sin[\Delta\varphi(t)] \tag{18}$$

with

$$\Delta\varphi(t) = \varphi(t) - \varphi(t - T). \tag{19}$$

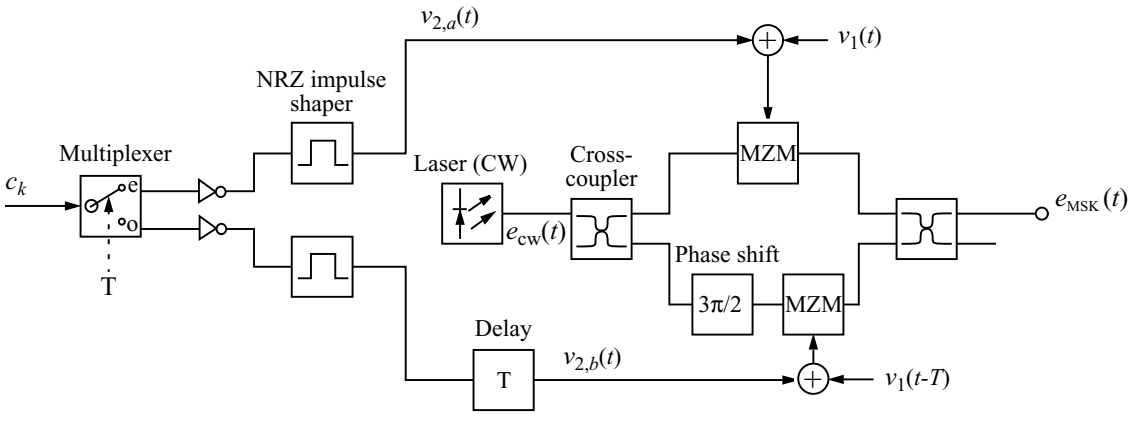

Figure 6. Optical MSK transmitter

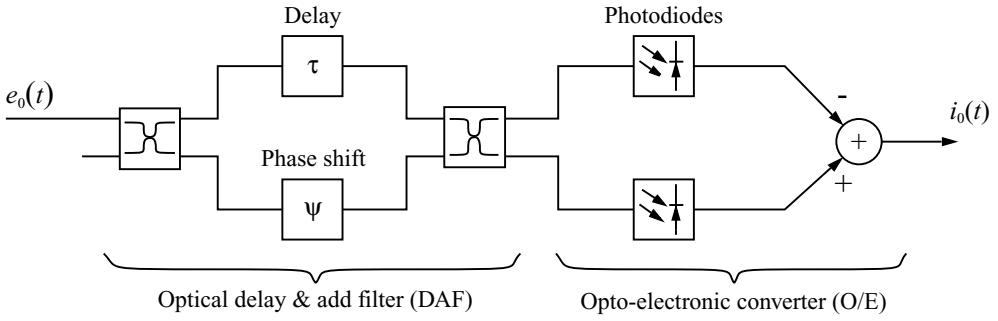

Figure 7. Optical MSK receiver

R is the responsivity of the photodiodes and K is a O/E conversion constant. At the sampling instants mT, $m \in \{0, \pm 1, \pm 2, \ldots\}$ the output current is

$$i_0(mT) = \pm 1 \cdot K \cdot R \cdot P \cdot A^2 \tag{20}$$

with the negative sign for bit '0' and the positive sign for bit '1'. Thus, a binary decision device with threshold 0 can be used to estimate the bit sequence d_k.

5. MSK PRECODER

The detected bit sequence d_k at the receiver output is not equal to the bit sequence c_k at the transmitter input. However, d_k is a function of c_k. In the following an MSK precoder will be derived such that the input to the precoder and the output of the receiver are equal. The task of the precoder is illustrated in Fig. 8. The cascade of MSK transmitter and receiver can be translated into the equivalent logic circuit in Fig. 9. It contains negated XOR gates, an inverter, and a delay element (memory). The multiplexer (MUX) at the output forwards either the upper (1) or the lower (0) input to the output depending on the clock signal t_k, alternating between 0 and 1. A state-transition diagram derived from the circuit in Fig. 9 is given in Fig. 10. The first digit of the state labels stands for the instantaneous value of the clock signal t_k and the second digit represents the output of the delay element c_{k-1}. The first digit in the transition labels is the input symbol c_k , and the second digit denotes the output symbol d_k. Further, the state-transition diagram can be transferred into a truth table (see Table 1). The MSK precoder function can be easily derived from Table 1. We find

$$c_k = t_k \cdot \overline{c_{k-1}} \cdot d_k + t_k \cdot c_{k-1} \cdot \overline{d_k} + \overline{t_k} \cdot \overline{c_{k-1}} \cdot \overline{d_k} + \overline{t_k} \cdot c_{k-1} \cdot d_k. \tag{21}$$

c_k is a function of c_{k-1}, the precoder input sequence d_k and an alternating clock signal t_k.

6. FEATURES OF MSK

6.1. Spectrum

First we present the spectrum of an MSK signal in comparison to the spectra of DBPSK and DQPSK in Fig. 11. In each case the bit rate is 10 Gbit/s and the signal power is identical. We assume that the electrical drive signals

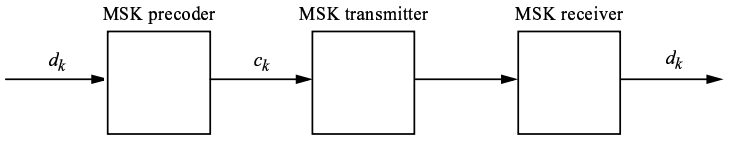

Figure 8. MSK precoder in series with the MSK transmitter and receiver

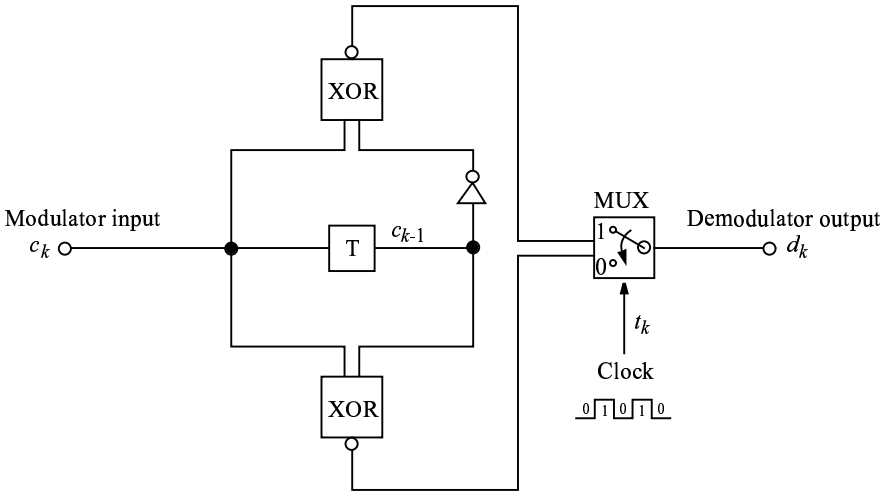

Figure 9. Logic circuit equivalent to cascade of MSK transmitter and receiver

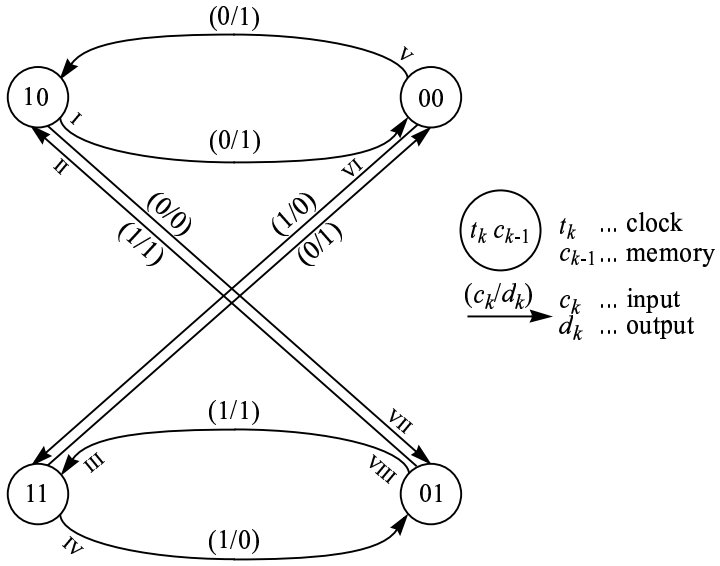

Figure 10. State-transition diagramm for equivalent circuit

Table 1. Truth table for state-transition diagram

Transition	Clock t_k	Input c_k	Memory c_{k-1}	Output d_k
I	1	0	0	0
II	1	1	0	1
III	1	0	1	1
IV	1	1	1	0
V	0	0	0	1
VI	0	1	0	0
VII	0	0	1	0
VIII	0	1	1	1

exhibits perfectly rectangular NRZ shape. (In the MSK case, $v_2(t)$ is a NRZ signal, whereas $v_1(t)$ of course is the triangular signal.) No optical filtering was applied. It can be seen that the main lobe of the MSK spectrum is narrower than the main lobe of the DBPSK spectrum. Also, for MSK more signal energy is contained in the main lobe compared to DBPSK. The side lobes of the MSK spectrum contain less energy than the side lobes of the DBPSK spectrum. MSK has a slightly broader main lobe than DQPSK. However, the side lobes of the MSK spectrum contain less energy. These spectral properties make MSK an interesting alternative to DBPSK and DQPSK for dense wavelength-division multiplexing (DWDM). With MSK individual channels can be spaced more closely.

6.2. Hardware complexity

Hardware complexity of the three modulation schemes is compared in Table 2. The MSK transmitter is similar to the DQPSK transmitter, whereas the MSK receiver is similar to the DBPSK reciver. Hardware amount of MSK lies in between DBPSK and DQPSK.

6.3. Impact of bandlimited electrical drive signal

In a real system, the electrical drive signals will not be of perfectly rectangular or triangular, because this would require infinite bandwidth. We investigated the proposed MSK scheme for finite bandwidth electrical drive signals. The results are shown in Fig. 12. The bit rate was chosen to 10 Gbit/s. The perfect rectangular or triangular signals have been filtered by 3rd order Bessel low-pass filters. The 3 dB bandwidths were set to 20 GHz, 30 GHz, and 40 GHz (Fig. 12(a)-(c)). The optical signals passed through an optical 3rd order Bessel band-pass filter with 3 dB bandwidth of 40 GHz. For comparison, Fig. 12(d) shows the case that the electrical drive signals are not band limited, but the optical filter is used. Fig. 12(e) shows the ideal MSK case with neither electrical nor optical filter. For all five cases it was assumed that the electrical receiver is described by a 3rd order Bessel low-pass filter with a 3 dB bandwidth of 20 GHz. The first column shows the triangular electrical drive signal. The greater the electrical bandwidth the sharper are the edges of the triangle. The spectra do not vary significantly. Only the first two side lobes become more distinct with increased bandwidth. The power of the

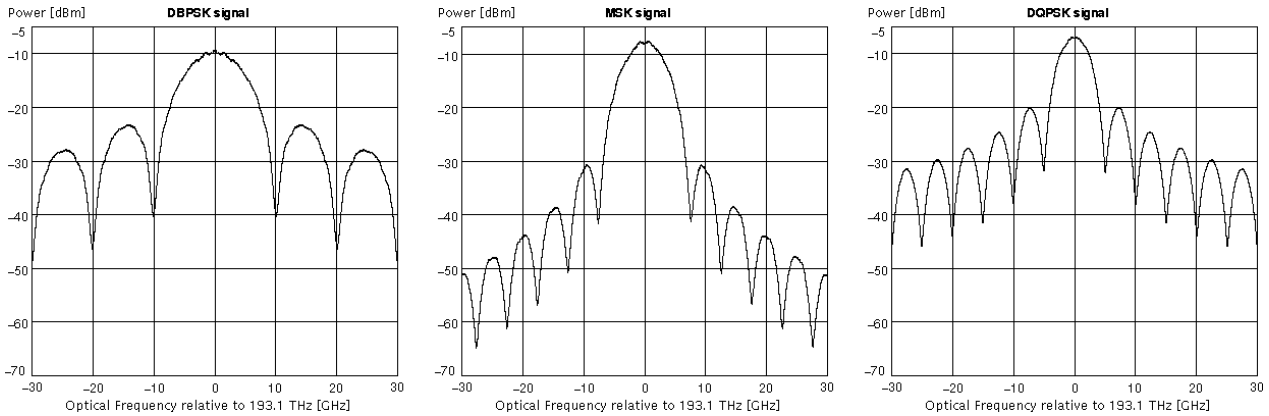

Figure 11. Spectra of DBPSK, MSK and DQPSK for 10 Gbit/s

Table 2. Comparison of hardware complexity for DBPSK, MSK, and DQPSK

	DBPSK	MSK	DQPSK
Precoder	yes	yes	yes
Duration of el. impulses at tx	T	2T	2T
MZMs at tx	1	2	2
DAFs at rx	1	1	2

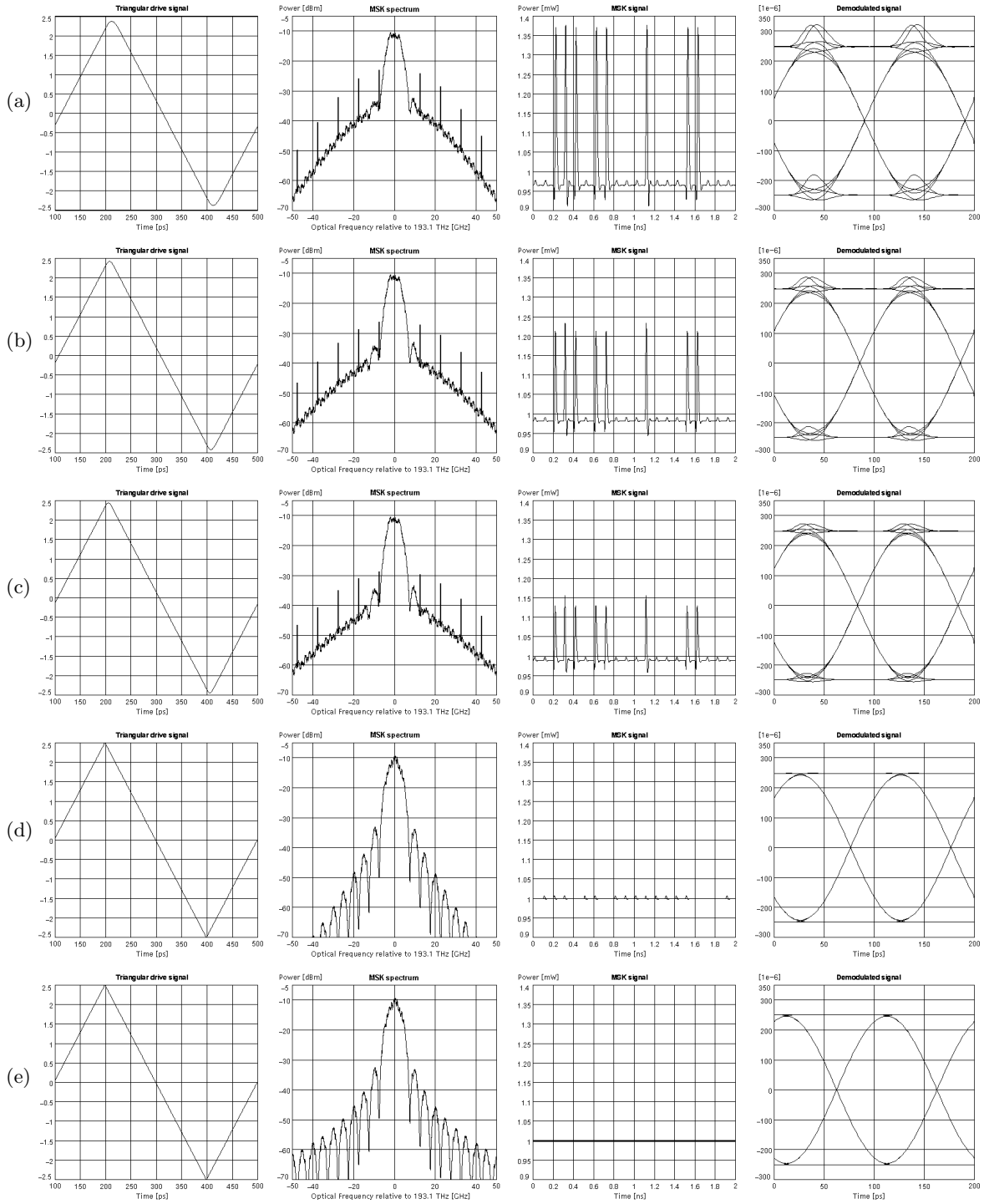

Figure 12. Effects of electrical and optical band limitation at transmitter:
(a) el. 3rd order Bessel low-pass (3 dB bandwidth 20 GHz), opt. 3rd order Bessel band-pass (3 dB bandwidth 40 GHz)
(b) el. 3rd order Bessel low-pass (3 dB bandwidth 30 GHz), opt. 3rd order Bessel band-pass (3 dB bandwidth 40 GHz)
(c) el. 3rd order Bessel low-pass (3 dB bandwidth 40 GHz), opt. 3rd order Bessel band-pass (3 dB bandwidth 40 GHz)
(d) no electrical band limitation, optical 3rd order Bessel band-pass (3 dB bandwidth 40 GHz)
(e) neither electrical nor optical band limitiation

optical time domain MSK signals exhibit more differences. They are shown in the third column for the time span $20T$. Obviously, for increasing bandwidth, the power variations decline. For electrical drive signals with infinite bandwidth and bandlimited optical signal (Fig. 12(d)), there are still some small power variations, whereas the ideal MSK signal in Fig. 12(e) shows constant power. The eye diagrams of the received signals in column 4 show, that the closer the triangular signal is approximated, the greater the eye opening is. Note, that even in the case of an ideal drive signal Fig. 12(e) the eye openeing is slightly decreased, because of the band limited receiver. The vertical eye-closing effect caused by band-limited electrical drive signals can be remedied by optical filtering after the transmitter. Fig. 13(c) shows that an optical tx filter yields a significantly greater vertical eye opening than without an optical tx filter (Fig. 13(a)). Also, the spectrum of the filtered signal (Fig. 13(d)) has a higher stopband attenuation than the unfiltered one (Fig. 13(b)). The reason for the improvement can be found in Fig. 14, which presents (a) the envelopes of the in-phase components, (b) the phases and (c) the instantaneous frequency offsets from the carrier for optically filtered and unfiltered MSK signals. Obviously, the curves for the filtered signal are smoother than for the unfiltered signal.

With simulations dispersion tolerance of MSK was investigated and compared to DBPSK. Fig. 15 shows eye opening penalties (EOP) vs. residual dispersion for both schemes. The bitrate of both systems was 10 Gbit/s, transmitters and receivers show 3rd order Bessel low-pass filter electrical characteristics with 20 GHz 3 dB-cut-off frequency. Both systems used optical 3rd order Bessel tx filters with 30 GHz 3 dB cut-off frequency and rx filters with 40 GHz 3 dB-cut-off frequency. As can be seen from Fig. 15, for small residual dispersion DBPSK has a slightly lower EOP than MSK. However, for residual dispersion above approximately 850 ps/nm MSK performs better than DBPSK. We have further found that the MSK eye remains open up to 2400 ps/nm, wheras the DBPSK eye is already totally closed at 1600 ps/nm. Note, that DBPSK generally has a higher dispersion tolerance than IM.

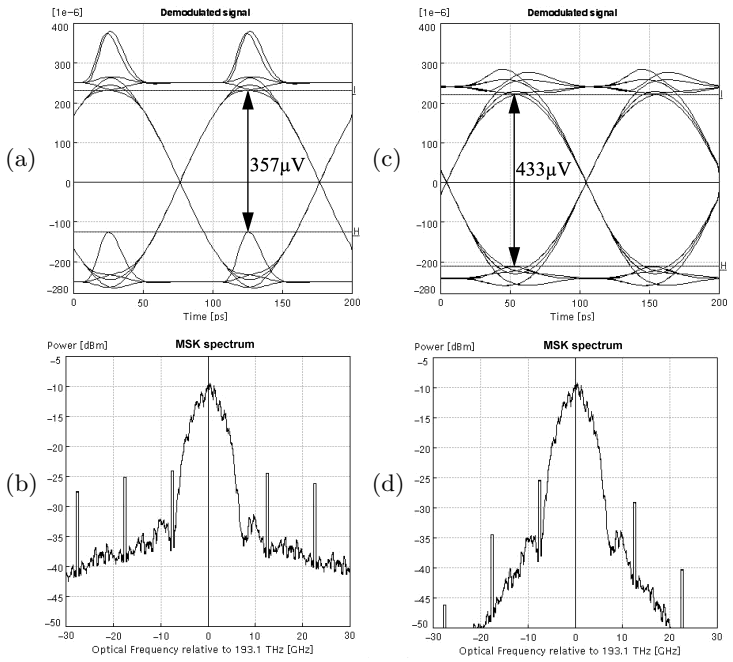

Figure 13. Impact of optical filtering at the transmitter on demodulated signal and MSK spectrum:
(a) eye diagram and (b) MSK spectrum without optical tx filter
(c) eye diagram and (d) MSK spectrum with optical 3rd order Bessel tx band-pass filter, 3 dB bandwidth 20 GHz

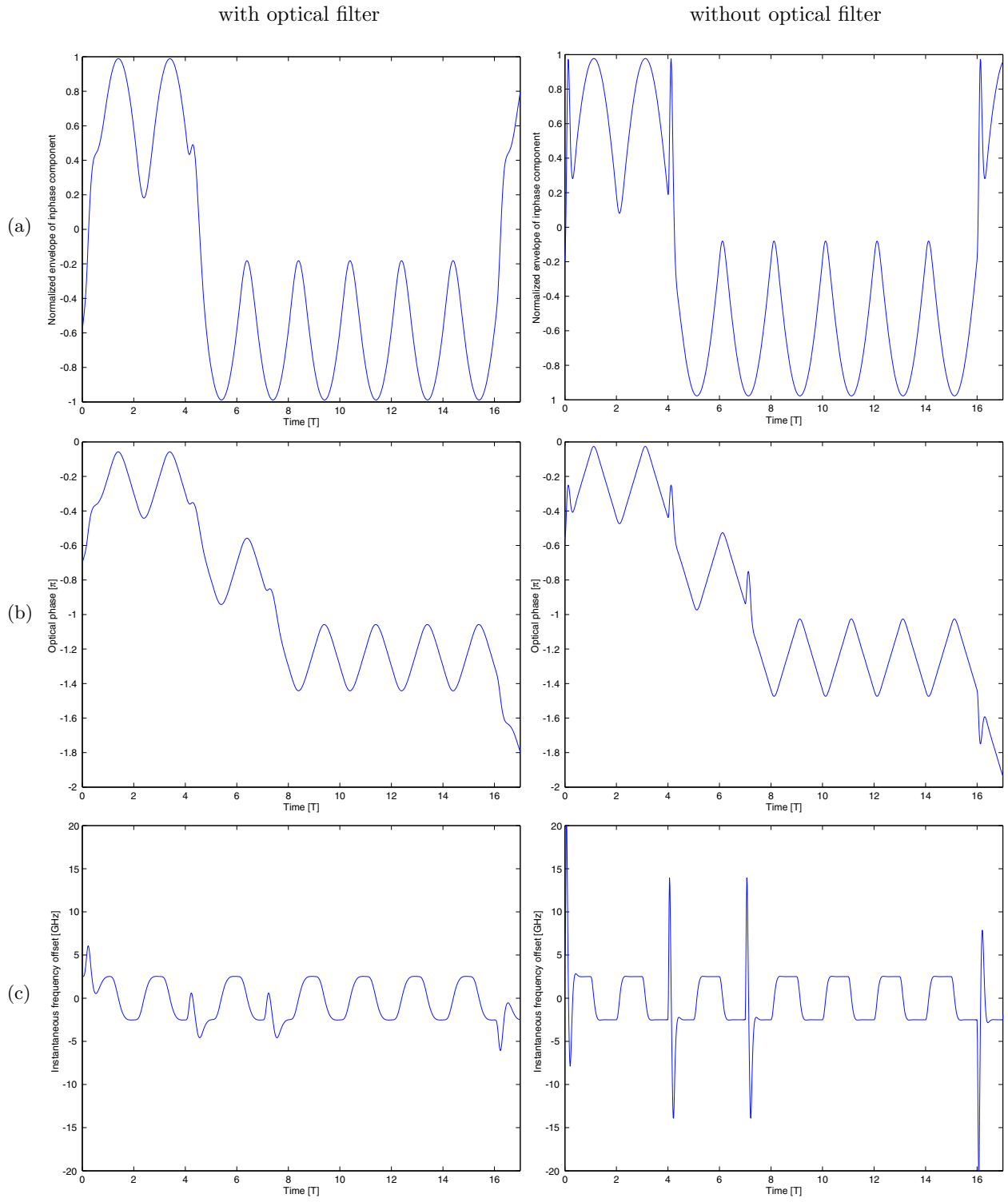

Figure 14. (a) Normalized envelope of in-phase component, (b) phase $\varphi(t)$, and (c) instantaneous frequency offset from carrier for optically filterd (left) and optically unfiltered (right) MSK signal with bandlimited electrical drive signals

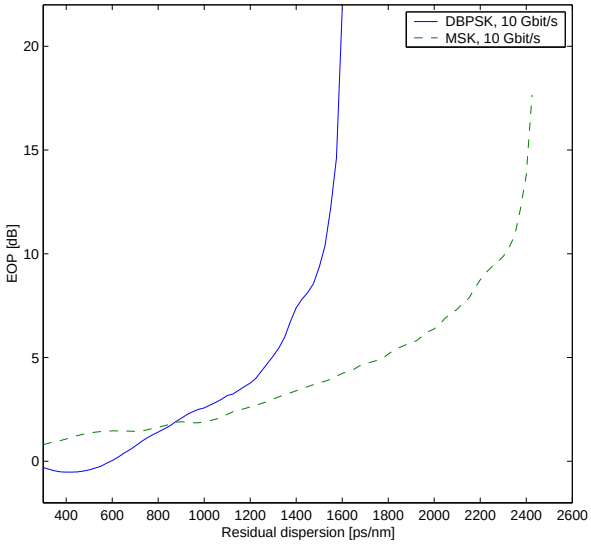

Figure 15. Normalized envelope of in-phase component, phase $\varphi(t)$, and momentary frequency offset from carrier for optically filterd (left) and optically unfiltered (right) MSK signal with bandlimited electrical drive signals

7. CONCLUSIONS

We have presented a new optical MSK scheme with precoder, modulator and demodulator. The transmitter is implemented as offset-QPSK using MZMs for impulse shaping. The receiver consists of a DAF and photodiodes for direct detection. We have shown by simulation that MSK is spectrally more efficient than DBPSK and mostly also DQPSK. This makes MSK an interesting candidate for DWDM systems. The hardware complexity of MSK lies in between DBPSK and DQPSK. Impact of electrical and optical band limitation was discussed. An optical band-pass filter at the transmitter increases the vertical eye opening of the demodulated signal. Dispersion tolerance of MSK was investigated and our simulation shows, that MSK has a significantly lower EOP than DBPSK for residual dispersion larger than about 850 ps/nm. Further investigation on the impact of fiber nonlinearities and other typical effects in optical transmission systems on MSK are necessary and in process.

ACKNOWLEDGMENTS

Parts of this work were funded by the German BMBF in the MultiTeraNet project.

REFERENCES

1. R. A. Griffin and A. C. Carter, "Optical differential quadrature phase-shift key (oDQPSK) for high capacity optical transmission," in *Proc. OFC 2002*, paper WX6.
2. M. Ohm and J. Speidel, "Quaternary optical ASK-DPSK and receivers with direct detection (ASK-DPSK/DD)," *IEEE Photonics. Tech. Lett.* **15**, pp. 159–161, January 2003.
3. M. Ohm and J. Speidel, "Differential optical 8-PSK with direct detection (8-DPSK/DD)," in *4. ITG-Fachtagung Photonische Netze*, *ITG-Fachbericht Photonische Netze*, pp. 177–181, May 2003.
4. R. Fritsch and J. Speidel, "OQ^{2}AM - optical QAM scheme with orthogonal polarization," in *4. ITG-Fachtagung Photonische Netze*, *ITG-Fachbericht Photonische Netze*, pp. 169–176, May 2003.
5. J. G. Proakis, *Digital Communications*, ch. 4. McGraw-Hill, New York, 4th ed., 2001.
6. M. Rohde, C. Caspar, N. Heimes, M. Konitzer, E.-J. Bachus, and N. Hanik, "Robustness of DPSK direct detection format in standard fibre WDM systems," *Electron. Lett.* **35**, pp. 1483–1484, August 2000.
7. *Photonic Modules Reference Manual*, Virtual Photonics, 2000.